STScI | SPACE TELESCOPE SCIENCE INSTITUTE

Instrument Science Report WFC3 2016-10

WFC3/UVIS EPER CTE Cycles Aug 2009 - Apr 2016

Harish Khandrika, Sylvia Baggett, Ariel Bowers

May 23, 2016

Abstract

This report summarizes the changes in Charge Transfer Efficiency (CTE) as determined by the Extended Pixel Edge Response (EPER) method. The results are derived from data acquired during Cycle 17 through Cycle 22 (August 2009-present). The EPER method uses large overscan regions obtained via a non-standard readout mode to measure CTE trails as a function of distance from the last row of illuminated science pixels. The CTE decline is steepest at the lowest signal values (160 e^- signal level) and more shallow at the highest signal levels (5000 e^-). We measure the evolution of CTE since the installation of WFC3; over 7 years the CTE has degraded by 0.07% for the lowest illumination level.

Introduction

Charge Transfer Efficiency (CTE) loss, an expected degradation in on-orbit CCDs, has been tracked in all HST CCD detectors: WFPC2 (e.g. Golimowski and Biretta 2010), STIS (Dixon 2011 and references therein) and ACS (Ubeda and Anderson 2012 and references therein). Damage to the silicon lattice by cosmic rays is the main cause of the degradation which directly affects photometric and astrometric precision on Hubble programs. The UV/optical channel (UVIS) of the Wide-Field Camera 3 (WFC3) instrument has also been affected by CTE loss. One method of monitoring this effect is the Extended Pixel Edge Response (EPER) technique (Bourque and Kozhurina-Platais 2013, Robberto 2007); it takes advantage of a special readout mode that provides a larger-than-normal overscan area (extended pixel region) within which to measure CTE trails. The internal flatfield lamp provides the stimulus.

In this paper we present analysis results of the on-orbit internal WFC3/UVIS EPER observations acquired for all data since cycle 17, including the most recent data from Cycles 21 and 22. This paper serves as an update to the previous UVIS EPER CTE measurements (Bourque and Kozhurina-Platais 2013, and references therein).

Data

UVIS EPER data were acquired through the programs listed in Table 1. For each proposal, short internal flat-field observations are taken in pairs with two different filters at various exposure times to achieve an specific illumination levels. The exposures and visit structures have been kept identical over the cycles to provide a stable dataset from which to measure the EPER CTE. The pair of EPER visits are outlined in Table 2.

Table 1: List of CTE EPER proposals.

Proposal ID	**Cycle**	**Principal Investigator**	**Frequency**
11924	17	Kozhurina-Platais	Once a month
12357	18	Kozhurina-Platais	Once a month
12691	19	Kozhurina-Platais	Once a month
13082	20	Bourque	Once a month
14011	21	Bowers	Every other month
14377	22	Khandrika	Every other month

Table 2: Observational parameters for a two-visit pair, where n is the first visit in the series and n+1 is the second.

Visit	**Image Type**	**Filter**	**Exp. Time (sec)**	**Illumination Level (e^-/pix)**
n	DARK	-	0.5	-
n	TUNGSTEN	F390M	9.2	160
n	TUNGSTEN	F390M	22.9	400
n+1	DARK	-	0.5	-
n+1	TUNGSTEN	F390W	6.4	800
n+1	TUNGSTEN	F438W	7.6	1600
n+1	TUNGSTEN	F438W	22.7	5000

Analysis and Results

UVIS EPER CTE analysis is based on the method outlined in Robberto 2007. Internal flatfields are taken in a special readout mode which generates extra overscan areas and the deferred charge due to CTE is then measured within that overscan (or extended pixel region).

Figure 1 shows the diagram of this unique readout mode. The overscan columns are first averaged in order to reduce the random Gaussian noise and improve the signal-to-noise. Some EPER observations can exhibit a low-level periodic electronic noise that varies from image to image; this extraneous signal is removed via sigma-clipping (Khozurina-Platais et al. 2011). The CTE is then calculated as the ratio of the total deferred charge in the overscan column average (S_D) to the charge level in the last column of science pixels (S_{LC}) multiplied by the number of pixel transfers in the CCD register (N_P). Figure 2 shows an example EPER image with overscan and CCD image area region.

$$\mathrm{CTE_{EPER}} = 1.0 - \frac{S_D}{S_{LC} \times N_P} \tag{1}$$

As noted in Khozurina-Platais et al. 2011, the CTE measurements show a power-law relationship between the CTE and signal level defined as follows:

$$\mathrm{CTE} = 1.0 - m \times (S_{LC})^{\rho} \tag{2}$$

Since CTE can also be characterized as charge transfer inefficiency (CTI = 1-CTE), we can write the above equation as

$$\log(\mathrm{CTI}) = \log(m) + \log(S_{LC}) \times \rho \tag{3}$$

This analysis technique has been run on all available on-orbit EPER data, from 2009 through Apr 2016. Figure 3 shows the measured EPER CTI as a function of signal level. Linear fits to each observation are plotted; different symbols correspond to the four different amps. The slope and intercept for the CTI, as shown in Equation 3 are plotted in Figure 3 as well. We find the same trends with the CTI over time as reported in Bourque and Kozhurina-Platais 2013: a stable CTI slope over time ($\rho = -0.68$) and increasing intercept of CTE over time.

In the current work, we have also improved the analysis procedure by correcting the data for cosmic rays. If CRs fall in the last science pixel row, they can increase the measured illumination level; this is likely to be a small effect given the relatively small chance of a CR landing in the last row. A larger effect can occur when they fall in the overscan area and introduce temporary additional charge in the EPER region which would lead to an artificially high measured CTE loss.

We investigated the outliers seen in figure 3, and discovered surprisingly large CTE tails due to an increased number of cosmic rays. The calculation of the CTE results in a CTE greater than 100% for amp C, and as a result causes the plotting program to be unable to plot the logarithm of the CTI (1-CTE) for all amps. Thus the outliers went unknown until this study, where the plotting program was converted to python, which replaces the errant value with a NAN and plots the remainder of the points. We attempted to grow the Cosmic Ray masks by extending the positions of the DQ flags to incorporate the CTE tails and while the value of the CTE does decrease, it still remains greater than one. Further investigation is required and will be one of the goals for future work.

The accumulated data up to November 2014 have been processed with the old method and all data accumulated to November 2015 have been processed with the new method. Figure 4 compares the results for the two methods for 160 e^- of illumination as a function

of time. The CR-corrected data show systematically better CTE than the uncorrected data, as expected, and there is somewhat less scatter in the CR-corrected data. Overall the CR correction seems to improve the CTE measurement and thus has been applied to all on-orbit (2009-2016) EPER images. The resulting plot of CTE as a function of time and illumination level is shown in Figure 4. As found previously, the CTE of the WFC3/UVIS detectors has continued to decline with time. Furthermore, as seen in past analyses as well, the fainter illumination levels have more CTE loss and steeper slopes than the brighter illumination levels (Anderson et al. 2012).

The EPER CTE decline has traditionally been modeled with a linear least-squares fit however with the addition of the new data, the decline is clearly non-linear, especially in the lower illumination rates. To determine if a different functional form would better match the data, we fit quadratic, log, linear, and double linear functions to the data. The curves for the 1600 e^- illumination level and the corresponding fit formulae are provided in Figure 6.

To identify the optimum date for transitioning from one linear fit to another in the double linear case, we performed a chi-squared test and located the MJD (Modified Julian Date) that minimizes the chi-squared for all curves. Figure 7 shows the chi-squared value for each MJD cutoff. As expected, the highest chi-squared values are encountered towards either the earliest or latest time period. The black points on the chart mark the location of minimum chi-squared for each illumination level, and the purple bar represents the median MJD corresponding to the minimum chi-squared values. This a transition date of MJD=56390 was chosen for the double linear fit.

Figure 8 shows the weighted residuals for each type of fit and the associated chi-squared and reduced chi-squared values for a 1600 electron illumination level. Table 3 also lists the chi-squared and minimum and maximum residuals for this illumination level. The largest residuals and chi-squared are for the linear fit, confirming it is not the best functional form to use to describe the time evolution for the EPER CTE data. The best fit of the four,with the lowest chi-squared and smallest residuals, is the quadratic fit. Weighted residuals for the double linear fit were computed with the transition date noted above, corresponding to the best match for all illumination levels, but the quadratic fit still matches the data best. This might indicate that the CTE decline is reducing or leveling off over time.

Summary

This report summarizes the behavior of the Charge Transfer Efficiency (CTE) as measured via the Extended Pixel Edge Response (EPER) method. The analysis procedure has been updated to include masking of cosmic rays and the new process applied to all on-orbit data (Cycle 17 through Cycle 22, 2009-2016) As expected, the CTE has 1) continued to decline with time and 2) is steeper for the fainter signal levels. We determine that the rate of decline is no longer well-matched by a linear fit but instead, is well fit by a quadratic function. This may indicate that the CTE decline is leveling off or reducing with time.

Acknowledgements

We would like to thank Matthew Bourque for his help with repairing and running the EPER monitoring script. We would also like to thank Dr. Gabriel Brammer for his careful and constructive review of our work and the ISR.

References

Anderson, J. et al. (2012). *The Efficacy of Post-Flashing for Mitigating CTE-Losses in WFC3/UVIS Images*. WFC3 report. Space Telescope Science Institute. URL: `http://www.stsci.edu/hst/wfc3/ins_performance/CTE/ANDERSON_UVIS_POSTFLASH_EFFICACY.pdf`.

Bourque, M. and V. Kozhurina-Platais (2013). *WFC3/UVIS EPER CTE Measurement: Cycles 19 and 20*. Instrument Science Report - WFC3. Space Telescope Science Institute.

Dixon, W.V. (2011). *Effects of CTE Degradation on Cycle 18 Observations with the STIS CCD*. Instrument Science Report - STIS. Space Telescope Science Institute.

Golimowski, D. and J. Biretta (2010). *The Dependence of WFPC2 Charge Transfer Efficiency on Background Illumination*. Instrument Science Report - WFPC2. Space Telescope Science Institute.

Khozurina-Platais, V. et al. (2011). *WFC3/UVIS EPER CTE Measurement: Cycles 17 and 28*. Instrument Science Report - WFC3. Space Telescope Science Institute.

Robberto, M. (2007). *UVIS CCD EPER CTE measurements performed during the April 2007 Ambient Calibration campaign (SMS UV02S01)*. Instrument Science Report - WFC3. Space Telescope Science Institute.

Ubeda, L. and J. Anderson (2012). *Study of the evolution of the ACS/WFC charge transfer efficiency*. Instrument Science Report - ACS. Space Telescope Science Institute.

Table 3: Various fits, residuals, and chi-squares for the different illumination levels

Illumination level	**Fit**	**Chi-squared**	**Residual Min**	**Residual Max**
5000 e-	Quadratic	8.843	-1.121	1.194
	Double Linear fit	9.589	-0.669	1.084
	Linear fit	41.81	-1.13	2.515
	Log fit	37.92	-1.095	2.442
1600 e-	Quadratic	10.22	-1.439	0.988
	Double Linear fit	12.65	-1.354	0.89
	Linear fit	56.47	-1.431	3.205
	Log fit	50.76	-1.426	3.031
800 e-	Quadratic	9.403	-0.692	1.731
	Double Linear fit	12.40	-0.952	1.498
	Linear fit	102.7	-1.838	4.525
	Log fit	92.16	-1.77	4.289
400 e-	Quadratic	11.02	-0.922	1.307
	Double Linear fit	20.00	-1.224	1.145
	Linear fit	135.9	-1.817	5.25
	Log fit	121.2	-1.74	4.989
160 e-	Quadratic	25.13	-1.36	1.547
	Double Linear fit	40.16	-1.757	1.789
	Linear fit	287.2	-2.967	9.258
	Log fit	256.1	-2.842	8.82

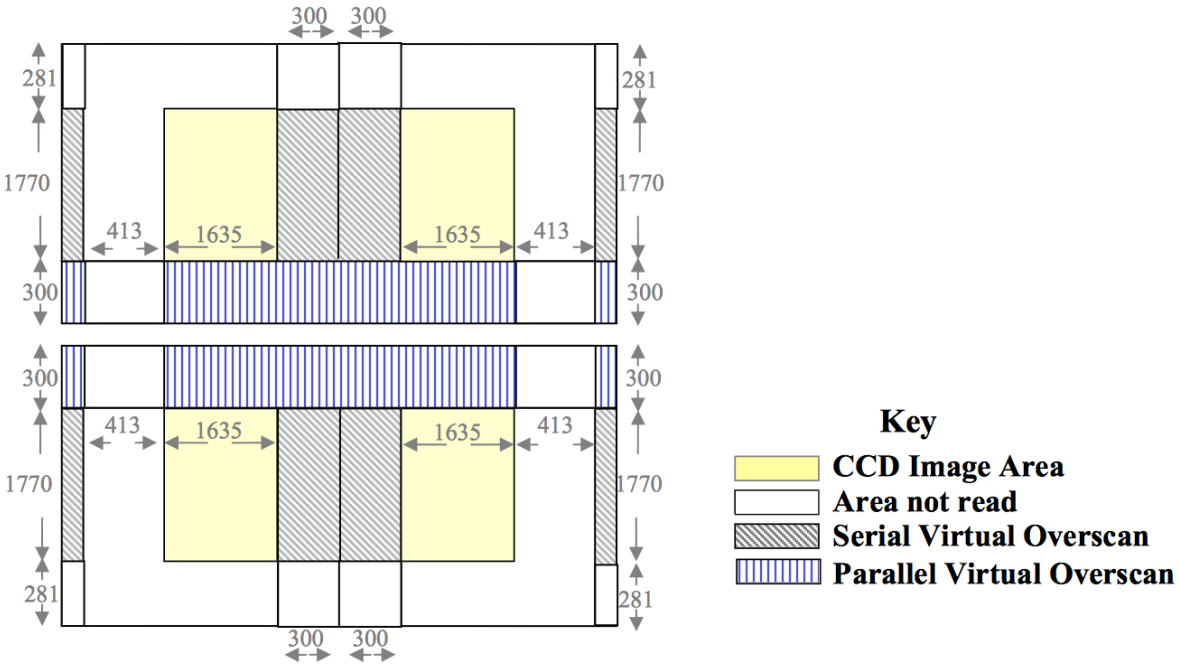

Figure 1: Diagram of the EPER readout mode as provided in Robberto 2007, Figure 2

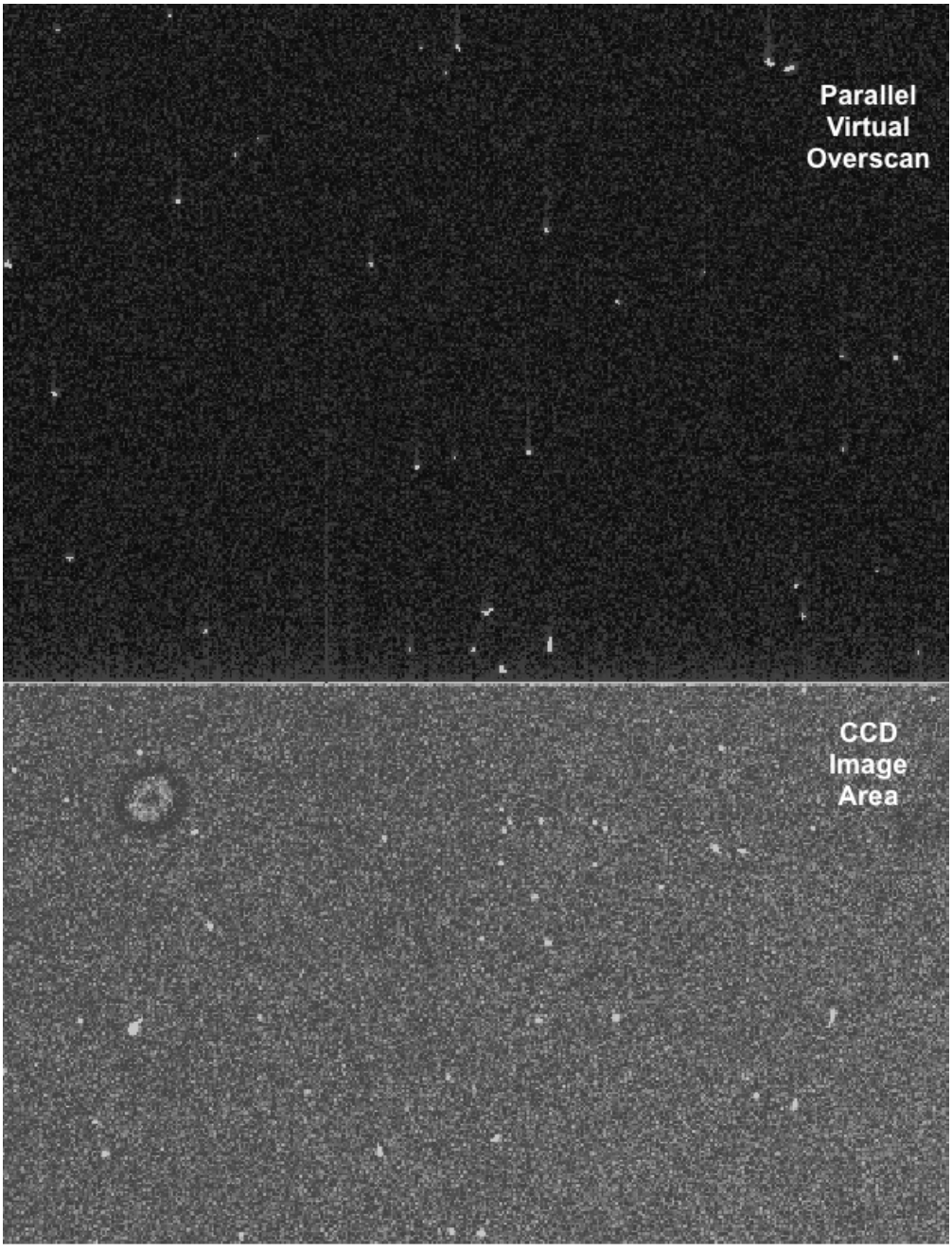

Figure 2: Example EPER image with the Parallel Virtual Overscan on top and a portion of the CCD image area on the bottom. Note the CTI tails leading into the overscan region from the image area

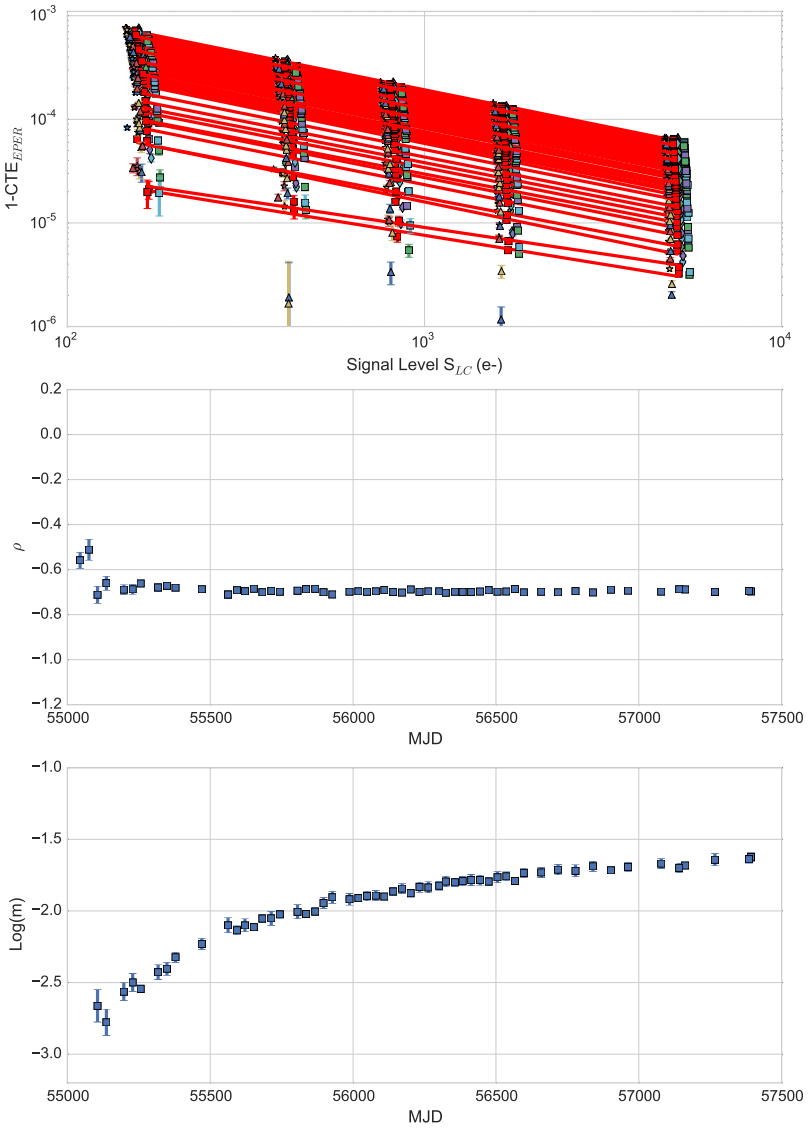

Figure 3: Top panel shows the CTI (1-CTE) versus the signal level in electrons (e^-) with a linear fit for each observation. Star, diamond, triangle, and square shapes represent each of the four amps: A,B,C,D respectively. The middle panel shows CTI slope versus time on a log-log scale. The bottom panel shows the CTI intercept as a function of time on a log-log scale

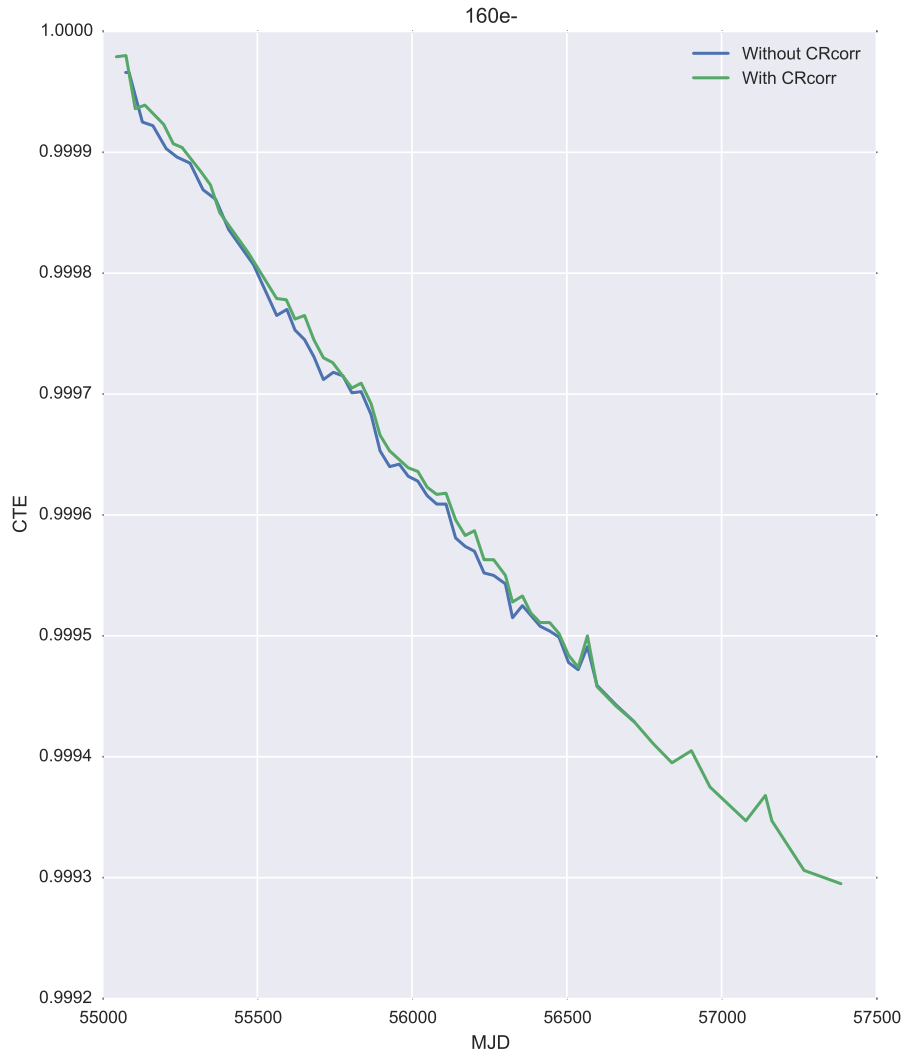

Figure 4: EPER CTE as a function of time for cosmic ray corrected data (green) and non-cosmic Ray corrected data (blue) for illumination level of 160 e^-. Note that newer data were not processed with the old method therefore the blue curve does not extend as far as the green curve.

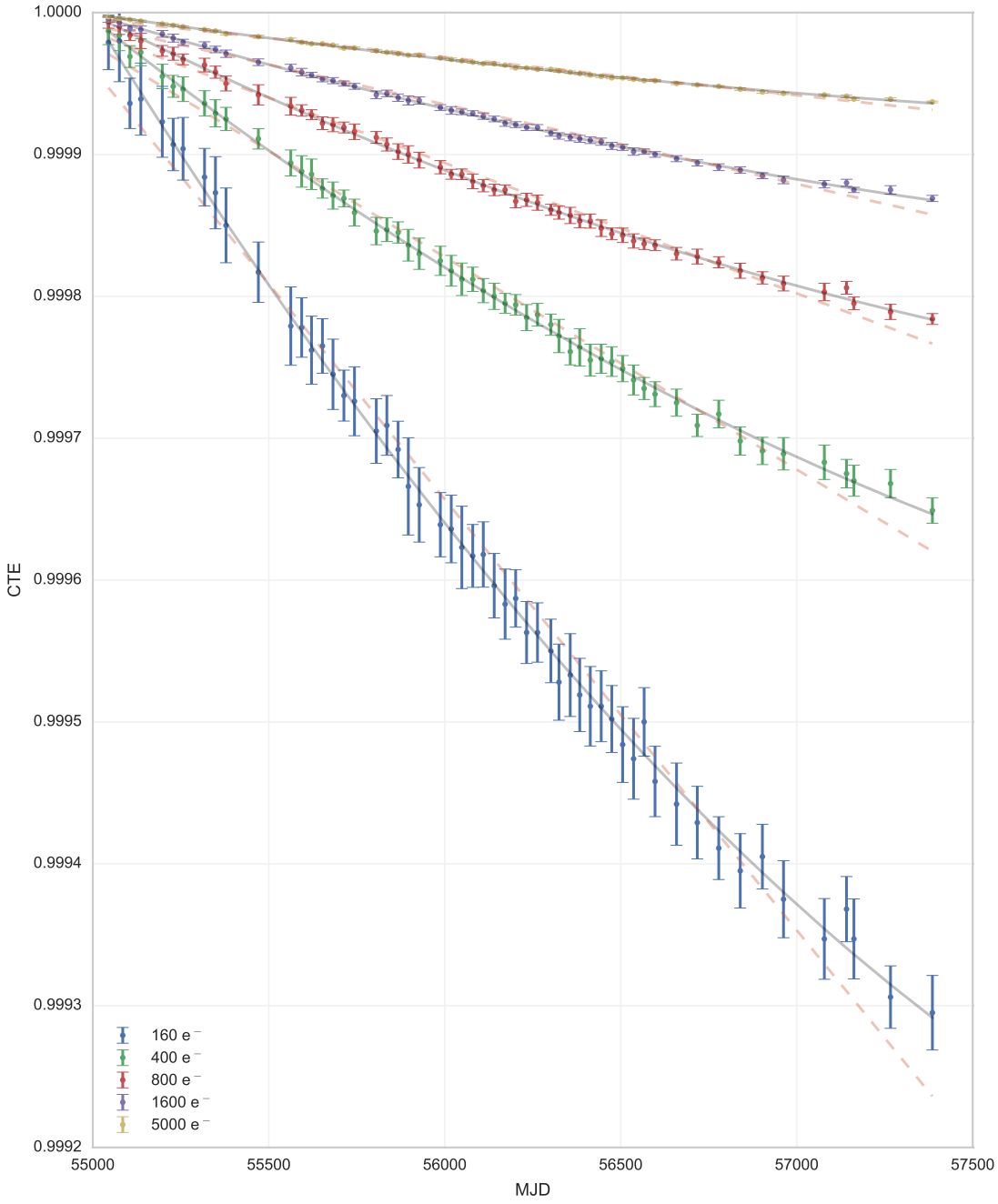

Figure 5: Decline of EPER CTE over time as a function of illumination level in electrons (e^-). A quadratic fit is overplotted over the points with a solid gray line and a linear fit is overplotted with a dashed orange line.

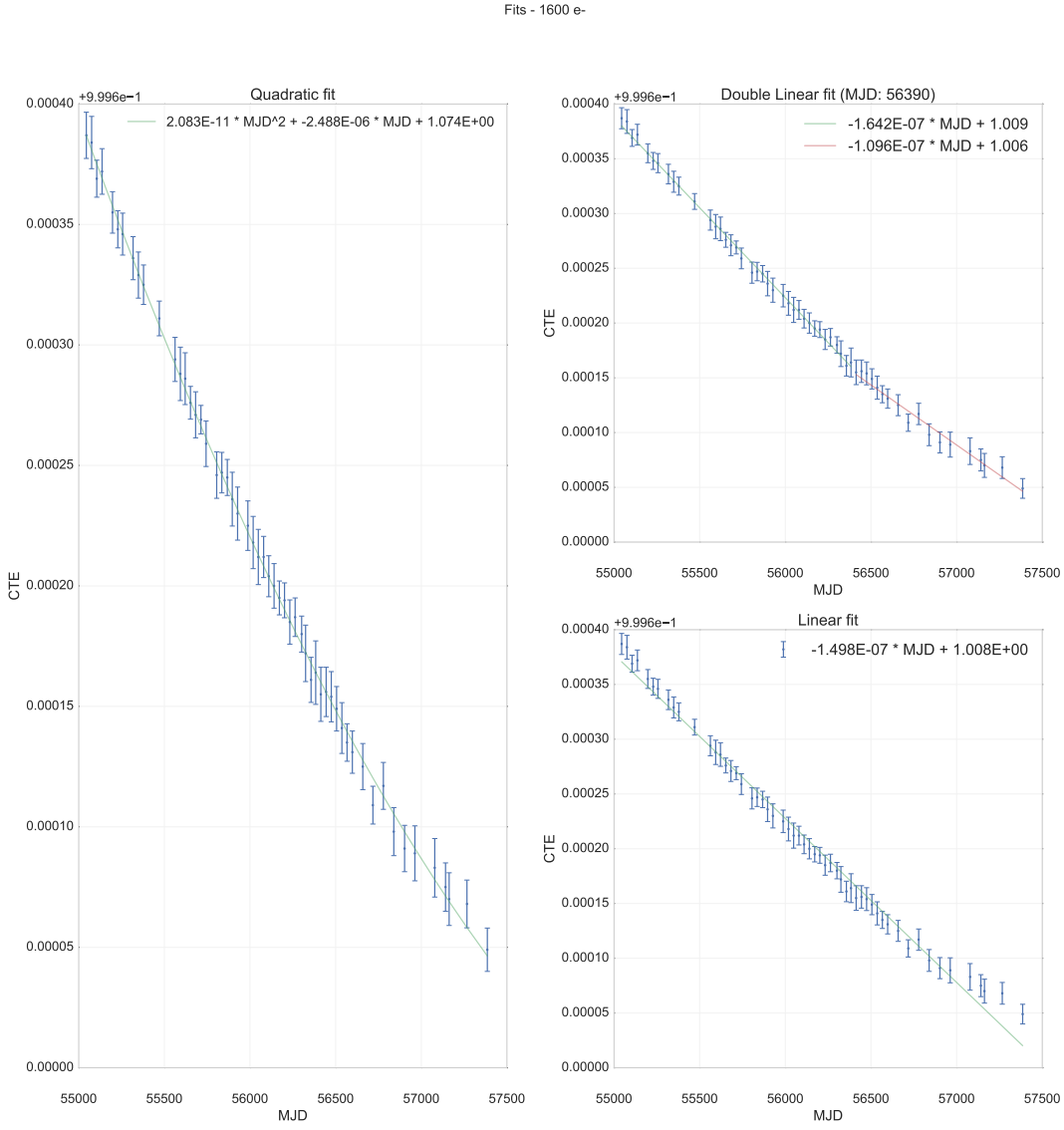

Figure 6: Quadratic, double linear, linear, and logarithmic fits to the 1600 e^- illumination level data. The fit formulae and coefficient values are noted within each panel along with the one-σ errors. For the double linear fit, MJD=56390 (April 08,2013) was used as the transition point.

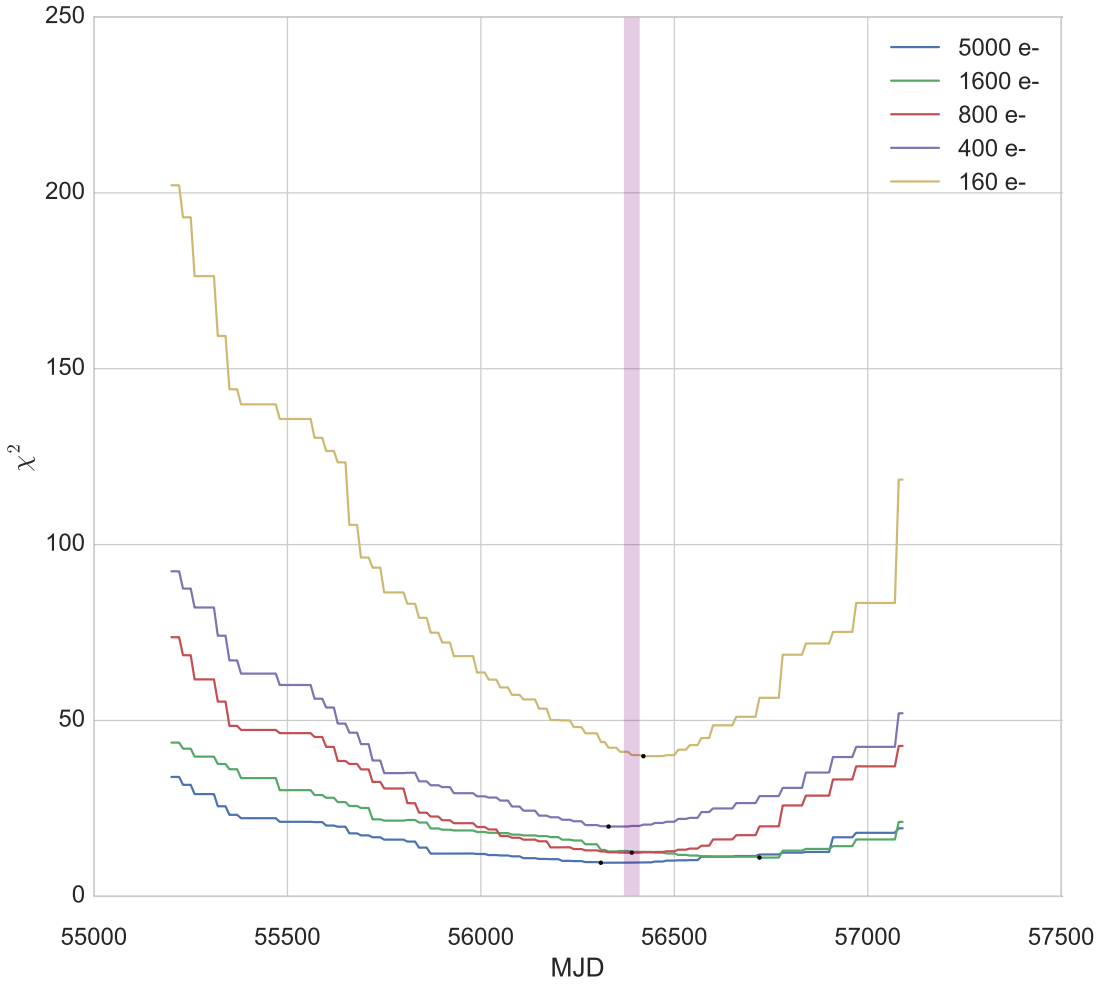

Figure 7: Chi-squared test results for the double linear fit. The pink vertical bar represents the median of the lowest chi-squared values (represented by black dots). The MJD corresponding to this is 56390.

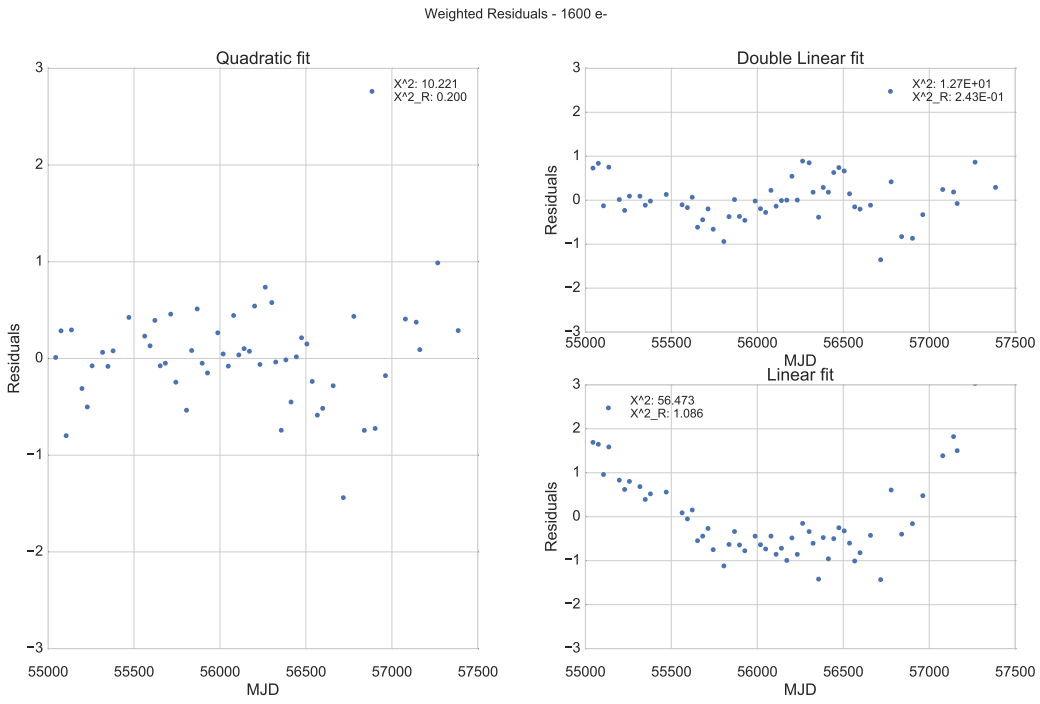

Figure 8: Residuals of the quadratic, double linear, linear, and logarithmic fits for the 1600 e^- signal level along with the equivalent chi-squared and reduced chi-squared values. The double linear fit is created using a 56390 MJD transition date.